Electronic properties of B-C-N ternary kagome lattices

Yuki Sakai, Susumu Saito, and Marvin L. Cohen

Phys. Rev. B **91**, 165434 — Published 29 April 2015

DOI: 10.1103/PhysRevB.91.165434

Electronic properties of B-C-N ternary kagome lattices

Yuki Sakai,[1,2,3] Susumu Saito,[2,4] and Marvin L. Cohen[1,5]

[1]*Department of Physics, University of California, Berkeley, California 94720, USA*

[2]*Department of Physics, Tokyo Institute of Technology, 2-12-1 Oh-okayama, Tokyo 152-8551, Japan*

[3]*Department of Applied Physics, The University of Tokyo, 7-3-1, Hongo, Bunkyo-ku, Tokyo 113-8656, Japan*

[4]*International Research Center for Nanoscience and Quantum Physics, Tokyo Institute of Technology, 2-12-1 Oh-okayama, Tokyo 152-8551, Japan*

[5]*Materials Sciences Division, Lawrence Berkeley National Laboratory, Berkeley, California 94720, USA*

(Dated: April 13, 2015)

Abstract

We investigate the electronic properties of boron-carbon-nitrogen (B-C-N) analogues of a recently proposed carbon kagome lattice [Chen *et al.*, Phys. Rev. Lett. 113, 085501 (2014)]. The B-C-N kagome lattices are constructed by replacing the carbon zigzag chains of the carbon kagome lattice with boron nitride zigzag chains. We use calculations of phonon dispersion curves to demonstrate the thermodynamic stabilities of the BCN and BC_4N kagome lattices. The B-C-N kagome lattices are wide-band gap semiconductors although the band gaps of the BCN and BC_4N kagome lattices are increased and reduced respectively compared with the carbon case. The reduction of band gap is found to be caused by a direct- to indirect-gap transition in the BC_4N kagome lattice.

I. INTRODUCTION

Carbon allotropes and boron nitride (BN) polymorphs have structural counterparts to one another. For example, well-known structural counterparts of graphite, carbon nanotubes, diamond, and hexagonal diamond are hexagonal BN, BN nanotubes, cubic BN, and wurtzite BN, respectively. Because of their structural similarities, covalently bonded boron-carbon-nitrogen (B-C-N) ternary compounds have attracted considerable interest for decades. Graphitic,[1–13] cubic,[14–26] and wurtzite[27–30] forms of B-C-N compounds with various compositions ($B_xC_yN_z$) have been intensively studied. Similarly, B-C-N ternary nanotubes have been investigated after the discovery of carbon and BN nanotubes.[31–47] These B-C-N materials generally exhibit intermediate structural and electronic properties of their parent carbon allotropes and BN polymorphs, and one can expect that their properties can be tuned by controlling the ratio of boron, carbon, and nitrogen atoms. Recently, monolayer materials of carbon (graphene) and BN (BN monolayer) have been fabricated.[48–51] These successful fabrications stimulate interest in a new class of B-C-N hybrid materials, which are weakly-bonded van der Waals heterostructures of graphene and BN monolayers.[52–60]

A new allotrope of carbon, the carbon kagome lattice, has been recently proposed based on theoretical calculations.[61,62] This carbon kagome lattice is composed of 4-fold coordinate carbon atoms although one of the bond angles is 60° [triangles can be seen in the top view in Fig. 1(a)]. The atomic configuration is alternatively regarded as three zigzag chains covalently bonded with each other. This carbon kagome lattice is thermodynamically stable in spite of its unusual geometry, and could be suitable for optical device applications because of its direct band gap (3.43 eV at the Γ point) comparable to ZnO and GaN, as well as having small carrier effective masses.

In this paper, we propose B-C-N ternary materials, B-C-N kagome lattices with structures analogous to the carbon kagome lattice. One or two of three carbon zigzag chains can be replaced with BN chains without introducing unfavorable boron-boron and nitrogen-nitrogen bonds [see Figs. 1(b) and 1(c)]. These BC_4N and BCN kagome lattices are dynamically stable according to our phonon calculations. The B-C-N kagome lattices are interesting because they are B-C-N materials which have carbon structural counterparts but do not have BN counterparts (BN kagome lattices must have boron-boron and nitrogen-nitrogen bonds), and they are different from the B-C-N materials mentioned above. We find a direct to indirect

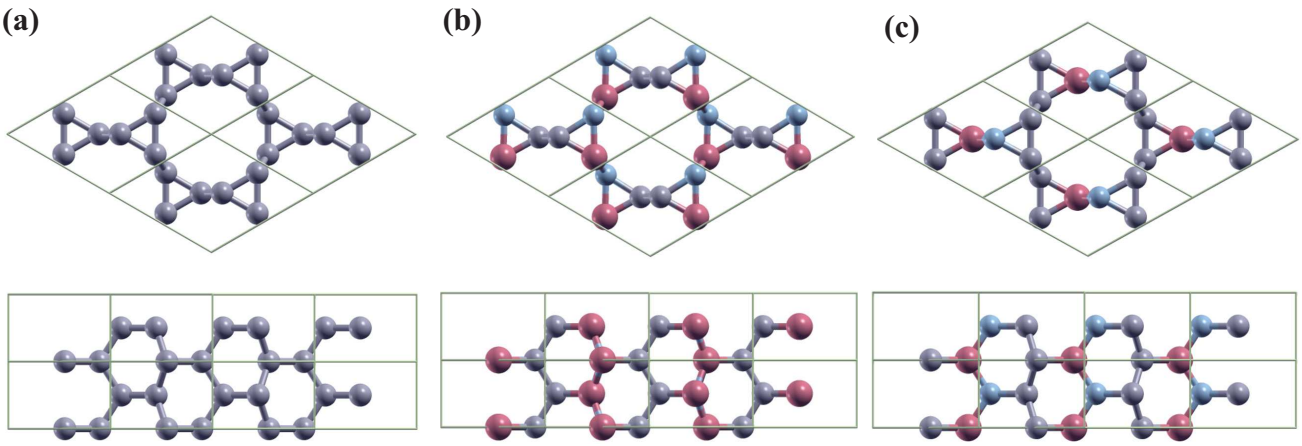

FIG. 1. (Color online) Top and side views of the crystal structures of (a) carbon, (b) BCN, and (c) BC_4N kagome lattices. Gray, pink, and green spheres represent carbon, boron, and nitrogen atoms, respectively. The carbon kagome lattice is composed of three carbon zigzag chains, one at the center of the unit cell, and two at the unit cell borders of the unit cell (see the top view). The carbon zigzag chains at the borders are substituted by BN in the BCN case while the center zigzag chain is replaced with BN in the BC_4N case. The unit cell of the BC_4N kagome lattice is slightly distorted from the hexagonal cell, and the angle between two in-plane lattice vectors is 122°. The distortion of the unit cell in the BCN kagome lattice is negligibly small (less than 0.1°).

gap transition caused by the BN substitution. The band gaps are found to increase and decrease respectively in BCN and BC_4N kagome lattices compared with the carbon kagome lattice by 0.46 and -0.16 eV, respectively.

II. COMPUTATIONAL METHODS

We adopt *ab initio* methods based on the density functional theory (DFT).[63,64] We use the Quantum ESPRESSO package for all the DFT calculations.[65] The Perdew-Burke-Ernzerhof (PBE) generalized gradient approximation functionals are used as exchange and correlation functionals for the DFT calculations.[66] We crosscheck band gaps with the hybrid functional developed by Heyd, Scuseria, and Ernzerhof (HSE).[67,68] The screening parameter of the HSE functional is 0.1058 a_0^{-1} where a_0 is the Bohr radius. The PBE optimized structures are used for the HSE calculations. Norm-conserving pseudopotentials of the Troullier-Martins type and a planewave basis set with a cutoff energy of 100 Ry are used.[69–72] The Brillouin zone

is sampled by $8 \times 8 \times 12$ and $36 \times 36 \times 54$ k-grids in structural optimization and density of states calculations, respectively. Phonon calculations are performed based on the density functional perturbation theory[73] with a $6 \times 6 \times 6$ q-grid. The XCrySDen code is used for the visualization of the DFT results.[74]

III. STRUCTURAL PROPERTIES

Structural parameters of carbon, BCN, and BC_4N kagome lattices are listed in Table I. Here we distinguish the bonds parallel to and intersecting with the rhombic face of the hexagonal unit cell (i.e. intra- and inter-triangle bonds). We refer to the former (latter) as planar (zigzag) bonds. The planar and the zigzag bonds can be also regarded as inter-zigzag chain and intra-chain bonds, respectively. The C-C and B-N zigzag bond lengths are comparable to those of the sp^2 and sp^3 bonds.[75] The longer bond-length tendency of B-N than C-C expands the unit cell volume as well as lattice constants of the BCN and BC_4N kagome lattices compared with those of the carbon kagome lattice. As can be seen from Table I, planar bonds tend to be longer than zigzag bonds. The planar B-C and C-N bonds have similar bond lengths (1.572 and 1.583 Å) while the planar B-N bond is slightly longer (1.591 Å) in the BCN case. Similarly, the planar C-C bond of the BC_4N kagome lattice (1.552 Å) is shorter than the B-C and C-N bond lengths (1.607 and 1.564 Å). The planar C-C bond of the carbon kagome lattice (1.528 Å) is the shortest among all the planar bonds. The long planar bond length implies a weaker inter-chain bonding of carbon-BN and BN-BN chains than the carbon-carbon chains.

To test the dynamical stabilities of the BCN and the BC_4N kagome lattices, we calculate phonon dispersion relations (see Fig. 2). We do not obtain any imaginary phonon frequencies in the phonon dispersion plot except for the acoustic modes at the Γ point, which is approximately 0.5 cm^{-1}. The magnitudes become smaller (about 0.01 cm^{-1}) when we use the local density approximation,[76,77] indicating the imaginary modes are caused by convergence problem. The bulk moduli of the B-C-N kagome lattices are comparable to that of the carbon kagome lattice (see Table I). The total energies of the BCN and BC_4N kagome lattices compared with their wurtzite forms (composed of carbon and BN bilayers) are 371 and 355 meV/atom, respectively. These values are also comparable to the total energy difference of the carbon kagome lattice and hexagonal diamond (253 meV/atom.) Therefore,

TABLE I. In-plane (a) and out-of-plane (c) lattice constants, unit cell volumes, bond lengths, and bulk moduli of carbon, BCN, and BC_4N kagome lattices. The bond types are distinguished by the planar and zigzag bonds. The lengths, the cell volumes, and bulk moduli are listed in Å, Å^3, and GPa, respectively.

	Carbon	BCN	BC_4N
a	4.445	4.544	4.550
c	2.524	2.542	2.529
C-C (planar)	1.528	-	1.552
C-C (zigzag)	1.495	1.485	1.488
B-N (planar)	-	1.591	-
B-N (zigzag)	-	1.508	1.509
B-C (planar)	-	1.572	1.607
C-N (planar)	-	1.583	1.564
Volume	43.2	45.4	44.5
Bulk modulus	324	275	298

we can conclude that these B-C-N kagome lattices should be dynamically as stable as the carbon kagome lattice. Note that the discontinuities of the phonon frequencies appear at the Γ point. Some of the Γ point frequencies depend on the direction of the approach to the Γ point, indicating the presence of the longitudinal- and transverse-optical mode splitting caused by the polar nature of the B-C-N kagome lattices.

IV. ELECTRONIC PROPERTIES

Figure 3 shows the band structures and densities of states of three kagome lattices. The carbon kagome lattice [Figs. 3(a) and 3(d)] is a direct gap semiconductor (2.30 eV at the Γ point) as previously reported.[61] The direct band gap at the Γ point of BCN and BC_4N are 3.45 and 2.84 eV, respectively. The amount of the BN substitution corresponds to the size of the band gap at the Gamma point in the B-C-N kagome lattices. We find that the conduction-band bottom state at the L point has lower energy than that of the Γ point in the BCN case as shown in Fig. 3(b) (2.65 eV indirect band gap). Interestingly, in the BC_4N

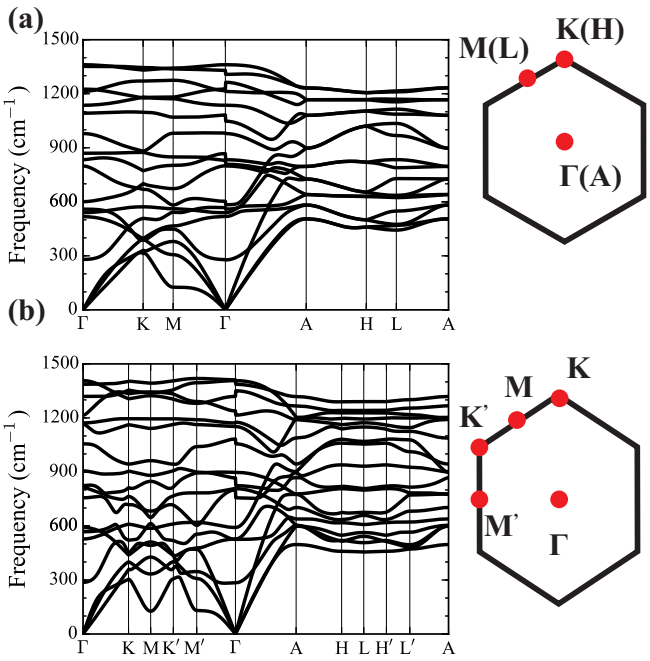

FIG. 2. (Color online) Phonon dispersion relations of (a) BCN, and (b) BC_4N kagome lattices (left panels). Schematic Brillouin zones projected to two dimensions are illustrated in the right panels. The BCN Brillouin zone is an ordinary hexagonal zone, but the Brillouin zone of the BC_4N kagome lattice is distorted with two long and four short sides (the distortion is exaggerated here). High-symmetry points are shown with red dots in the Brillouin zone figures with their corresponding names of the hexagonal Brillouin zone. The subscripts S and L for the M and L points denote short and long sides of the first Brillouin zone of the BC_4N kagome lattices. The A, H, and L in the parenthesis represent high-symmetry points at $k_z = 0.5 \times 2\pi/c$. The label convention of high-symmetry points at $k_z = 0.5 \times 2\pi/c$ is similar for the BC_4N Brillouin zone.

case the fundamental gap value is even reduced compared with the carbon case (2.06 eV indirect band gap). The conduction-band bottom state of the BC_4N kagome lattice is at the $L_{\rm L}$ point, and the highest valence band state is slightly shifted from the Γ point toward the K point [see Fig. 3(c)].

The HSE/PBE band gaps and PBE carrier effective masses are listed in Table II. The use of HSE does not qualitatively affect the result above, while the HSE band gap of the carbon kagome lattice is 3.30 eV at the Γ point, which is 1 eV higher than the PBE result. The direct band gap at the Γ point of the BCN and BC_4N kagome lattices are 4.43 and 3.88 eV, respectively. The L ($L_{\rm L}$) point state is still the lowest conduction-band state in

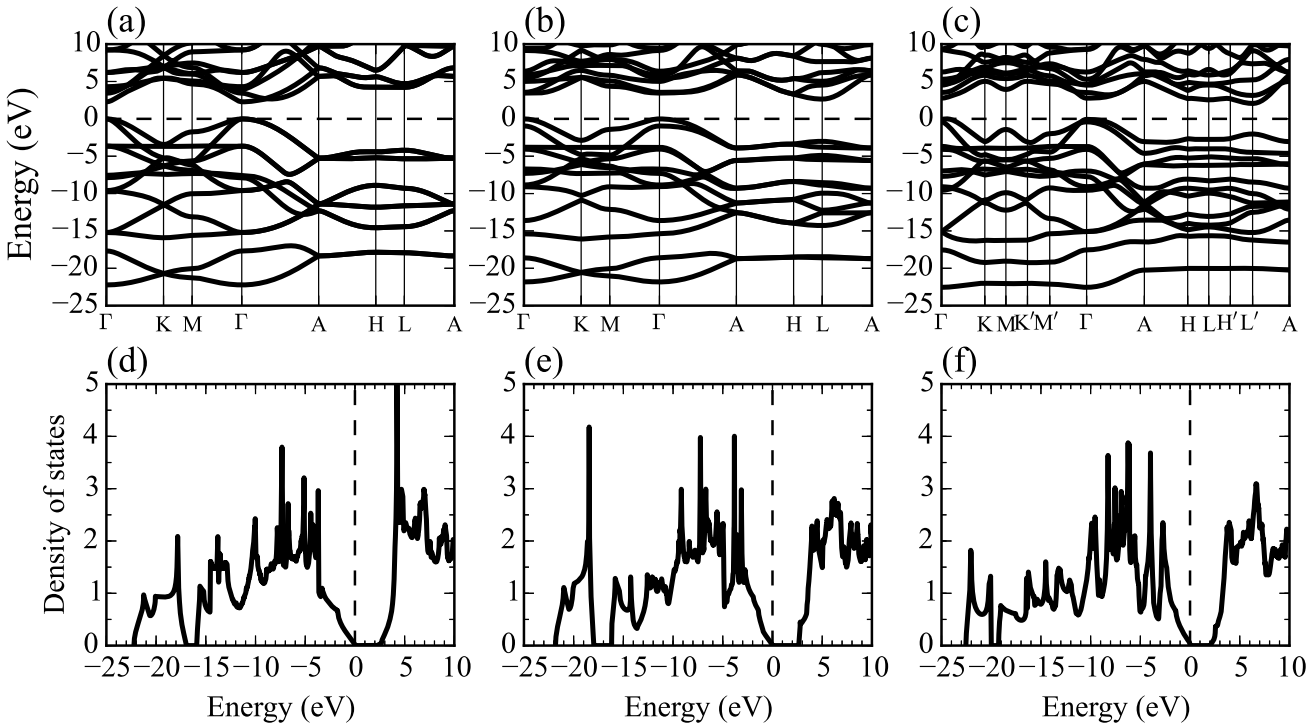

FIG. 3. PBE Band structures of (a) carbon, (b) BCN, and (c) BC_4N kagome lattices, and The dashed lines (energy references) indicate the top of the valence bands. The Brillouin zones and high-symmetry points are schematically illustrated in Fig. 2. Densities of states of (d) carbon, (e) BCN, and (f) BC_4N kagome lattices.

the BCN (BC_4N) kagome lattice, and the HSE indirect band gap is 3.76 (3.14) eV. The hole and electron effective masses of the BC_4N kagome lattice along the a-axis computed with the PBE functionals are 0.24 m_0 ($\Gamma^* \to K$ direction) and 0.20 m_0 ($L_{\rm L} \to A$ direction) respectively, where m_0 is the mass of a free electron. These values are still comparable to those of the carbon kagome lattice with hole and electron masses of 0.12 and 0.17 m_0 respectively, along the $\Gamma \to K$ direction. Therefore, the BC_4N kagome lattice would be a useful wide band gap semiconductor with light carriers.

In order to investigate further the effect of the BN substitution on the electronic structures, we discuss the characters of the Kohn-Sham wavefunctions in the following. We first consider the characters of the highest valence-band wavefunctions of the Γ point of carbon, BCN, and BC_4N kagome lattices [see Figs. 4(a), 4(b), 4(c), respectively]. The characters of the highest valence-band wavefunctions of the BCN and the BC_4N kagome lattices are qualitatively similar to those of the carbon kagome lattice. In the BCN case, the amplitude

TABLE II. Band gaps (E_g in eV) and in-plane electron/hole effective masses (m_e/m_h in terms of the free electron mass) of the three kagome lattices. The valence-band-top and conduction-band-bottom k-points are represented in the parentheses of the E_g. The direction of the calculation of the effective mass is also indicated in the parentheses. Light and heavy hole effective masses are listed in the carbon case because of the degeneracy.

	Carbon	BCN	BC_4N
E_g (PBE)	2.30 ($\Gamma \to \Gamma$)	2.65 ($\Gamma \to L$)	2.06 ($\Gamma^* \to L_{\rm L}$)[a]
E_g (HSE)	3.30 ($\Gamma \to \Gamma$)	3.76 ($\Gamma \to L$)	3.14 ($\Gamma^* \to L_{\rm L}$)[a]
m_e	0.17 ($\Gamma \to K$)	0.21 ($L \to A$)	0.20 ($L_{\rm L} \to A$)
m_h	0.12, 0.28 ($\Gamma \to K$)	0.30 ($\Gamma \to K$)	0.24 ($\Gamma^* \to K$)

[a] The Γ^* indicates the point on the Γ-K line very close to the Brillouin zone center.

at the planar B-N bond is relatively small compared with the planar B-C and N-C bonds. This wavefunction character can be related to the fact that planar B-N bond has a longer bond length (see Table I). Similarly, the amplitude of the wavefunction at the C-C bond is large compared with the B-C and N-C bonds in the BC_4N case, resulting from the bond length differences discussed in Sec. III.

Next we discuss the lowest conduction band wavefunctions which significantly affect the electronic properties of the BCN and the BC_4N kagome lattices. Figure 5 describes the conduction-bottom Kohn-Sham wavefunctions at the L ($L_{\rm L}$ for the BC_4N case) point. The L point wavefunction of the carbon kagome lattice is localized two-dimensionally as shown in Fig. 5. This localized nature is consistent with its almost flat band dispersion around the L point [see Fig. 3(a)]. In contrast, the wavefunction spreads more to the space between two nearest-neighbor boron atoms, and enhances the band dispersion in the zigzag-chain direction in the BCN and BC_4N cases [Figs. 5(b) and 5(c)]. This should contribute to the lowered energy of the L (L') point state of the BCN (BC_4N) kagome lattice, and results in the indirect band gap.

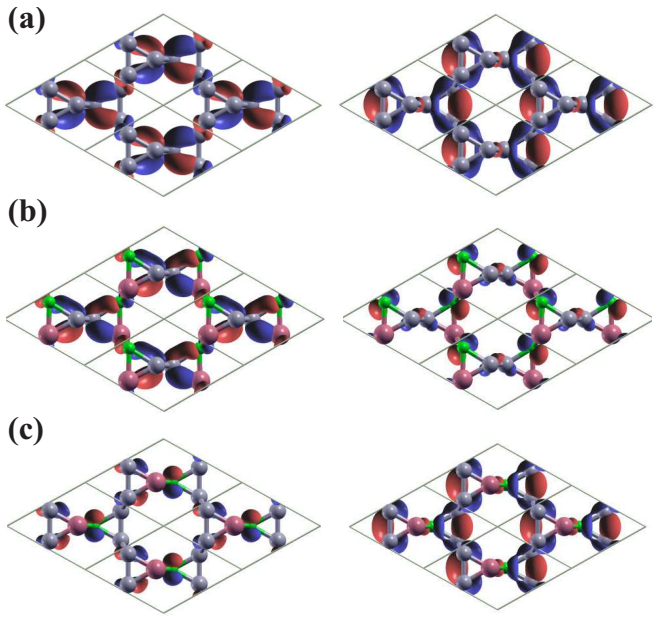

FIG. 4. (Color online) Top views of Kohn-Sham wavefunction at the Γ point of (a) carbon, (b) BCN, and (c) BC_4N kagome lattices. The red and blue isosurfaces represent plus and minus signs of the Kohn-Sham wavefunctions. The isosurfaces represent 10 % of the maximum amplitude of the wavefunctions. The left panels are the highest valence-band state while the right panels are second highest states. These states are degenerate in the carbon kagome lattice, and the degeneracy is lifted in the BCN and the BC_4N cases because of symmetry reduction. The atomic color scheme is the same as Fig. 1.

V. SUMMARY

We propose the design of BCN and BC_4N ternary kagome lattices and investigated their properties by using an *ab initio* calculation method based on DFT. These B-C-N kagome lattices are composed of interconnected one-dimensional carbon and BN zigzag chains, and are found to be dynamically stable. We also find that the band gap increases and decreases from the carbon kagome lattice in the BCN and BC_4N kagome lattices, respectively, and that the BCN and the BC_4N kagome lattices are both indirect gap semiconductors with the gap values of 3.76 and 3.14 eV, respectively in the HSE calculations. The highest valence Kohn-Sham wavefunction at the Γ point of the B-C-N kagome lattices are qualitatively similar to the carbon case. On the other hand, the wavefunction at the conduction band minimum have sizable amplitude along the zigzag chains in both BCN and BC_4N cases in

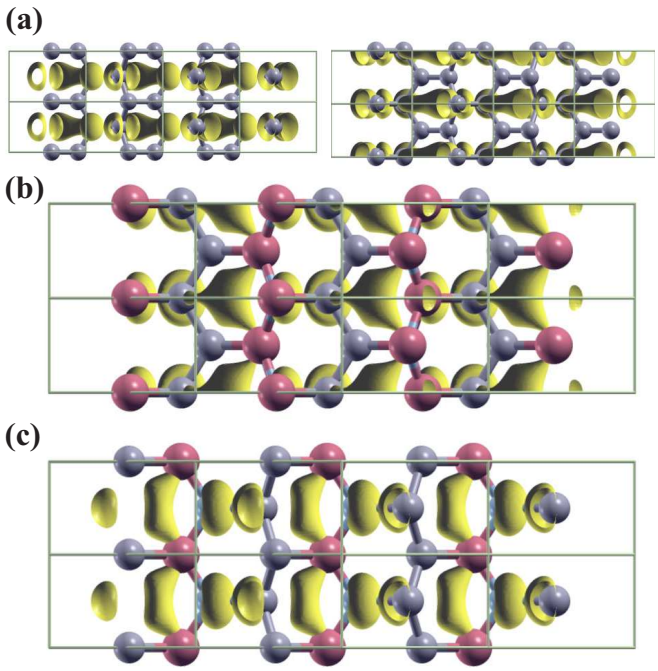

FIG. 5. (Color online) Side views of the Kohn-Sham wavefunctions of the lowest conduction states of (a) carbon, (b) BCN, and (c) BC_4N kagome lattices. The L point wavefunctions are illustrated for the carbon and BCN kagome lattices whereas the L_L point state is described for the BC_4N case. Two wavefunctions are plotted in (c) because the L point wavefunction of the carbon kagome lattice is doubly degenerated. The yellow isosurfaces represent 10 % of the maximum amplitude of the wavefunctions. The atomic color scheme is the same as Fig. 1.

contrast to a planar wavefunction of the carbon kagome lattice. The lowering of the energy of this dispersive state results in the indirect band gap of the B-C-N kagome lattices.

We suggest that these B-C-N kagome lattices could be promising wide gap light-elemental materials with light carrier effective masses. In addition, the fabrication of the B-C-N kagome lattices is expected to have little phase segregation of carbon and BN phases since a pure BN kagome lattice should be unstable because of the existence of boron-boron and nitrogen-nitrogen bonds. Therefore, the B-C-N kagome lattices should be more stable than other B-C-N materials which have BN structural analogues.

ACKNOWLEDGMENTS

Numerical calculations were partly carried out on the TSUBAME2.0 supercomputer in the Tokyo Institute of Technology. This work was supported by NSF Grant No. DMR-10-1006184, and the theory program at the Lawrence Berkeley National Laboratory through the Office of Basic Science, US Department of Energy under Contract No. DE-AC02-05CH11231. YS acknowledges financial support from Japan Society for the Promotion of Science (JSPS, 12J08928). SS acknowledges the financial support by Grant-in-Aid for Scientific Research from JSPS (No. 25107005), Global COE Program of MEXT Japan through the Nanoscience and Quantum Physics Project of the Tokyo Institute of Technology, and MEXT Elements Strategy Initiative to Form Core Research Center through Tokodai Institute for Element Strategy. We thank Yuanping Chen and Shengbai Zhang for useful discussions.

---

[1] A. R. Badzian, S. Appenheimer, T. Niemyski, and E. Olkusnik, in *Proceedings of the third international conference on chemical vapor deposition*, Vol. 3 (1972).

[2] R. B. Kaner, J. Kouvetakis, C. E. Warble, M. L. Sattler, and N. Bartlett, Mater. Res. Bull. **22**, 399 (1987).

[3] A. Y. Liu, R. M. Wentzcovitch, and M. L. Cohen, Phys. Rev. B **39**, 1760 (1989).

[4] M. Kawaguchi, T. Kawashima, and T. Nakajima, Chem. Mater. **8**, 1197 (1996).

[5] M. O. Watanabe, S. Itoh, T. Sasaki, and K. Mizushima, Phys. Rev. Lett. **77**, 187 (1996).

[6] A. Perrone, A. P. Caricato, A. Luches, M. Dinescu, C. Ghica, V. Sandu, and A. Andrei, Appl. Surf. Sci. **133**, 239 (1998).

[7] Y. Chen, J. C. Barnard, R. E. Palmer, M. O. Watanabe, and T. Sasaki, Phys. Rev. Lett. **83**, 2406 (1999).

[8] R. Gago, I. Jiménez, J. M. Albella, and L. J. Terminello, Appl. Phys. Lett. **78**, 3430 (2001).

[9] I. Shimoyama, Y. Baba, S. Tetsuhiro, K. G. Nath, M. Sasaki, and K. Okuno, J. Vac. Sci. Tech. A **21**, 1843 (2003).

[10] M. N. Uddin, I. Shimoyama, Y. Baba, T. Sekiguchi, and M. Nagano, J. Vac. Sci. Tech. A **23**, 497 (2005).

[11] Z. Pan, H. Sun, and C. Chen, Phys. Rev. B **73**, 193304 (2006).

[12] R. Torres, I. Caretti, R. Gago, Z. Martín, and I. Jiménez, Diamond Relat. Mater. **16**, 1450 (2007).

[13] I. Shimoyama, Y. Baba, and T. Sekiguchi, Carbon **71**, 1 (2014).

[14] A. R. Badzian, Mater. Res. Bull. **16**, 1385 (1981).

[15] S. Nakano, M. Akaishi, T. Sasaki, and S. Yamaoka, Chem. Mater. **6**, 2246 (1994).

[16] E. Knittle, R. B. Kaner, R. Jeanloz, and M. L. Cohen, Phys. Rev. B **51**, 12149 (1995).

[17] T. Komatsu, M. Nomura, Y. Kakudate, and S. Fujiwara, J. Mater. Chem. **6**, 1799 (1996).

[18] Y. Tateyama, T. Ogitsu, K. Kusakabe, S. Tsuneyuki, and S. Itoh, Phys. Rev. B **55**, R10161 (1997).

[19] V. L. Solozhenko, D. Andrault, G. Fiquet, M. Mezouar, and D. C. Rubie, Appl. Phys. Lett. **78**, 1385 (2001).

[20] H. Sun, S.-H. Jhi, D. Roundy, M. L. Cohen, and S. G. Louie, Phys. Rev. B **64**, 094108 (2001).

[21] Y. Zhao, D. W. He, L. L. Daemen, T. D. Shen, R. B. Schwarz, Y. Zhu, D. L. Bish, J. Huang, J. Zhang, G. Shen, J. Qian, T. W. Zerda, D. W. He, L. L. Daemen, T. D. Shen, R. B.Schwarz, Y. Zhu, D. L. Bish, J. Huang, J. Zhang, G. Shen, J. Qian, and T. W. Zerda, J. Mater. Res. **17**, 3139 (2002).

[22] Y. Zhang, H. Sun, and C. Chen, Phys. Rev. Lett. **93**, 195504 (2004).

[23] E. Kim, T. Pang, W. Utsumi, V. L. Solozhenko, and Y. Zhao, Phys. Rev. B **75**, 184115 (2007).

[24] H. Dong, D. He, T. S. Duffy, and Y. Zhao, Phys. Rev. B **79**, 014105 (2009).

[25] V. P. Filonenko, V. A. Davydov, I. P. Zibrov, V. N. Agafonov, and V. N. Khabashesku, Diamond Relat. Mater. **19**, 541 (2010).

[26] X. Zhang, Y. Wang, J. Lv, C. Zhu, Q. Li, M. Zhang, Q. Li, and Y. Ma, J. Chem. Phys. **138**, 114101 (2013).

[27] X. Luo, X. Guo, Z. Liu, J. He, D. Yu, B. Xu, Y. Tian, and H.-T. Wang, Phys. Rev. B **76**, 092107 (2007).

[28] Y. Li, W. Fan, H. Sun, X. Cheng, P. Li, X. Zhao, and M. Jiang, J. Phys. Chem. C **114**, 2783 (2010).

[29] T. Zhu and S. P. Gao, Euro. Phys. J. B **85**, 1 (2012).

[30] Q. Fan, Q. Wei, C. Chai, M. Zhang, H. Yan, Z. Zhang, J. Zhang, and D. Zhang, Comp. Mater. Sci. **97**, 6 (2015).

[31] S. Iijima, Nature (London) **354**, 56 (1991).

[32] Y. Miyamoto, A. Rubio, M. L. Cohen, and S. G. Louie, Phys. Rev. B **50**, 4976 (1994).

[33] A. Rubio, J. L. Corkill, and M. L. Cohen, Phys. Rev. B **49**, 5081 (1994).

[34] O. Stephan, P. M. Ajayan, C. Colliex, P. Redlich, J. M. Lambert, P. Bernier, and P. Lefin, Science **266**, 1683 (1994).

[35] Z. Weng-Sieh, K. Cherrey, N. G. Chopra, X. Blase, Y. Miyamoto, A. Rubio, M. L. Cohen, S. G. Louie, A. Zettl, and R. Gronsky, Phys. Rev. B **51**, 11229 (1995).

[36] P. Redlich, J. Loeffler, P. M. Ajayan, J. Bill, F. Aldinger, and M. Rühle, Chem. Phys. Lett. **260**, 465 (1996).

[37] Y. Zhang, H. Gu, K. Suenaga, and S. Iijima, Chem. Phys. Lett. **279**, 264 (1997).

[38] R. Sen, B. C. Satishkumar, A. Govindaraj, K. R. Harikumar, G. Raina, J.-P. Zhang, A. K. Cheetham, and C. N. R. Rao, Chem. Phys. Lett. **287**, 671 (1998).

[39] J. Yu, J. Ahn, S. F. Yoon, Q. Zhang, B. Gan, K. Chew, M. B. Yu, X. D. Bai, and E. G. Wang, Appl. Phys. Lett. **77**, 1949 (2000).

[40] F. Piazza, J. E. Nocua, A. Hidalgo, J. De Jesús, R. Velázquez, B. L. Weiss, and G. Morell, Diamond Relat. Mater. **14**, 965 (2005).

[41] S. Y. Kim, J. Park, H. C. Choi, J. P. Ahn, J. Q. Hou, and H. S. Kang, J. Am. Chem. Soc. **129**, 1705 (2007).

[42] S. Enouz-Védrenne, O. Stéphan, M. Glerup, J.-L. . L. Cochon, C. Colliex, and A. Loiseau, J. Phys. Chem. C **112**, 16422 (2008).

[43] K. Raidongia, D. Jagadeesan, M. Upadhyay-Kahaly, U. V. Waghmare, S. K. Pati, M. Eswaramoorthy, and C. N. R. Rao, J. Mater. Chem. **18**, 83 (2008).

[44] Z. Xu, W. Lu, W. Wang, C. Gu, K. Liu, X. Bai, E. Wang, and H. Dai, Adv. Mater. **20**, 3615 (2008).

[45] M. Matos, S. Azevedo, and J. R. Kaschny, Solid State Commun. **149**, 222 (2009).

[46] T. A. Souza, M. R. A. Silva, and A. C. M. Carvalho, Phys. Proc. **28**, 84 (2012).

[47] A. C. M. Carvalho, C. G. Bezerra, J. A. Lawlor, and M. S. Ferreira, J. Phys.: Condens. Matter **26**, 015303 (2014).

[48] A. Nagashima, N. Tejima, Y. Gamou, T. Kawai, and C. Oshima, Phys. Rev. B **51**, 4606 (1995).

[49] A. Nagashima, N. Tejima, Y. Gamou, T. Kawai, and C. Oshima, Phys. Rev. Lett. **75**, 3918 (1995).

[50] K. S. Novoselov, A. K. Geim, S. V. Morozov, D. Jiang, Y. Zhang, S. V. Dubonos, I. V. Grig-

orieva, and A. A. Firsov, Science **306**, 666 (2004).

[51] K. S. Novoselov, D. Jiang, F. Schedin, T. J. Booth, V. V. Khotkevich, S. V. Morozov, and A. K. Geim, Proc. Nat. Acad. Sci. USA **102**, 10451 (2005).

[52] J. Sławińska, I. Zasada, P. Kosiński, and Z. Klusek, Phys. Rev. B **82**, 085431 (2010).

[53] A. Ramasubramaniam, D. Naveh, and E. Towe, Nano Lett. **11**, 1070 (2011).

[54] Y. Sakai, T. Koretsune, and S. Saito, Phys. Rev. B **83**, 205434 (2011).

[55] Y. Sakai and S. Saito, J. Phys. Soc. Jpn. **81**, 103701 (2012).

[56] L. Britnell, R. V. Gorbachev, R. Jalil, B. D. Belle, F. Schedin, A. Mishchenko, T. Georgiou, M. I. Katsnelson, L. Eaves, S. V. Morozov, N. M. R. Peres, J. Leist, A. K. Geim, K. S. Novoselov, and L. A. Ponomarenko, Science **335**, 947 (2012).

[57] G. Gao, W. Gao, E. Cannuccia, J. Taha-Tijerina, L. Balicas, A. Mathkar, T. N. Narayanan, Z. Liu, B. K. Gupta, J. Peng, Y. Yin, A. Rubio, and P. M. Ajayan, Nano Lett. **12**, 3518 (2012).

[58] S. J. Haigh, A. Gholinia, R. Jalil, S. Romani, L. Britnell, D. C. Elias, K. S. Novoselov, L. A. Ponomarenko, A. K. Geim, and R. Gorbachev, Nature Mater. **11**, 764 (2012).

[59] A. K. Geim and I. V. Grigorieva, Nature (London) **499**, 419 (2013).

[60] Y. Sakai, S. Saito, and M. L. Cohen, Phys. Rev. B **89**, 115424 (2014).

[61] Y. Chen, Y. Y. Sun, H. Wang, D. West, Y. Xie, J. Zhong, V. Meunier, M. L. Cohen, and S. B. Zhang, Phys. Rev. Lett. **113**, 085501 (2014).

[62] O. Leenaerts, B. Schoeters, and B. Partoens, Phys. Rev. B **91**, 115202 (2015).

[63] P. Hohenberg and W. Kohn, Phys. Rev. **136**, 864 (1964).

[64] W. Kohn and L. J. Sham, Phys. Rev. **140**, 1133 (1965).

[65] P. Giannozzi, S. Baroni, N. Bonini, M. Calandra, R. Car, C. Cavazzoni, D. Ceresoli, G. L. Chiarotti, M. Cococcioni, I. Dabo, A. Dal Corso, S. de Gironcoli, S. Fabris, G. Fratesi, R. Gebauer, U. Gerstmann, C. Gougoussis, A. Kokalj, M. Lazzeri, L. Martin-Samos, N. Marzari, F. Mauri, R. Mazzarello, S. Paolini, A. Pasquarello, L. Paulatto, C. Sbraccia, S. Scandolo, G. Sclauzero, A. P. Seitsonen, A. Smogunov, P. Umari, and R. M. Wentzcovitch, J. Phys.: Condens. Matter **21**, 395502 (2009).

[66] J. P. Perdew, K. Burke, and M. Ernzerhof, Phys. Rev. Lett. **77**, 3865 (1996).

[67] J. Heyd, G. E. Scuseria, and M. Ernzerhof, J. Chem. Phys. **118**, 8207 (2003).

[68] J. Heyd, G. E. Scuseria, and M. Ernzerhof, J. Chem. Phys. **124**, 219906 (2006).

[69] J. Ihm, A. Zunger, and M. L. Cohen, J. Phys. C Solid State Phys. **12**, 4409 (1979).

[70] M. L. Cohen, Physica Scripta Volume T **1**, 5 (1982).

[71] N. Troullier and J. L. Martins, Phys. Rev. B **43**, 1993 (1991).

[72] S. G. Louie, S. Froyen, and M. L. Cohen, Phys. Rev. B **26**, 1738 (1982).

[73] S. Baroni, S. de Gironcoli, A. Dal Corso, and P. Giannozzi, Rev. Mod. Phys. **73**, 515 (2001).

[74] A. Kokalj, Comput. Mater. Sci. **28**, 155 (2003).

[75] The sp^2 (sp^3) bond length of carbon and BN calculated by using the present method are 1.42 (1.55) Å and 1.45 (1.57) Å, respectively.

[76] D. M. Ceperley and B. J. Alder, Phys. Rev. Lett. **45**, 566 (1980).

[77] J. P. Perdew and A. Zunger, Phys. Rev. B **23**, 5048 (1981).